Modal analysis and cutoff condition of a double-clad archimedean spiral shaped lightguide

RAM JATAN[a], RAM JANMA[b*], NARENDRA KUMAR[c], VIVEK SINGH[d]
[a]*Department of Physics, Bhanmati Smarak Mahavidyalaya, Ambedkarnagar 224210, UP, India*
[b]*Department of Physics, University Institute of Engineering and Technology, Chhatrapati Shahu Ji Maharaj University, Kanpur 208024, UP, India*
[c]*Department of Physics, CASH, Mody University of Science and Technology, Lakshmangarh 332311, Sikar, Rajasthan, India*
[d]*Department of Physics, Banaras Hindu University, Varanasi 221005, UP, India*

A simple analytical approach, based on scalar wave approximation, is employed to study the modal propagation characteristics of a new type of double-clad optical waveguide with an Archimedean spiral shaped cross-section. By using the boundary conditions under the weak-guidance approximation in appropriate orthogonal coordinates, for the proposed structure, we obtain a modal eigen value equation. By solving the equation, we plot dispersion curves and comparing these curves, numerical results based on cutoff frequencies and the number of modes, are discussed. As we increase the inner cladding width, the cutoff V-value also increases and waveguide offers a single mode up to V=13.8. An attempt has been made to compare our results obtained for doubly clad optical waveguide with a single clad waveguide having the cross-section of the same shape under similar conditions. It is noted that the double-clad Archimedean spiral waveguide provides an additional degree of freedom to control the cutoff frequencies and monomode operation, where the inner cladding width can tailor the cutoff conditions within a certain limit.

1. Introduction

Optical waveguides with different core-geometries have been analysed during the past decades, and unconventional waveguides have aroused great renewed interest in exploring a wide variety of such core cross-sections. One of the reasons of studying non-circular cross-section in a waveguide is to investigate the effect of distortion in the usual circular cross-section; however such distortion may not always be of symmetrical nature. In 1969, Marcatili [1] first analyzed the modal dispersion features of a rectangular core guiding structure with an analytical solution, whereas Goell [2] demonstrated dispersion characteristics of the rectangular waveguide using numerical and computer based calculations. Many no-circular waveguides with a variety of characteristics, having immense scope in integrated optics, have been analyzed [3-15].

The propagation characteristic of waveguide can be highly affected by introducing claddings of new materials [16-19]. Waveguides with more than one cladding layers, e.g. doubly clad M-profile and W-profile waveguides are found to be of great importance in research. Such double-clad waveguides [20-22] control their propagation characteristics offering some additional degree of freedom. Investigators have already proposed many optical waveguides with double layer or multilayered structures.

Although the unconventional core-geometries offer a number of applications, there are a few limitations for

tailoring propagation characteristics dynamically in time that can be overcome by using smart materials like chiral, liquid crystal and plasma [22]. Among them, single mode fibers [23-26] have great advantages in communication that can also be achieved by using double-clad waveguide with smart unconventional structures. The basic advantages of these type of waveguide is to have low dispersion over a wide wavelength range and also attractive for high-bit-rate light wave communication system [22].

Song and Leonhardt [27] have employed and demonstrated the ray-optics approach to calculate the single mode conditions of rectangular waveguides faster than those compared with the physical-optics. It offers visualized-oriented approach to analyze the propagation through three-dimensional waveguides, whose results are in a very good agreement with those obtained by the researchers with vectorial computer simulation techniques.

In recent, Grote and Bassett [28] have also suggested a waveguide design using negative high refractive-index substrates, where they propose that such geometry can be adapted for any high-index substrate material leading to offer platforms for nonlinear photonics. Kawakami *et al.* [29] determined the bending loss of a doubly clad slab waveguide in which the core has the largest refractive index, and the inner cladding has the lowest and demonstrated the drastic reduction in bending losses by inserting low-index inner claddings between the core and

the outer cladding. They determined bending-loss formulas of a multilayer planar optical waveguide on the basis of continuation of wave functions without solving the complicated eigen value equation.

In this article, the authors propose a new type of unconventional double-clad optical lightguide having Archimedean shaped cross-section, whose theoretical understanding such as, modal cutoff condition and propagation properties are determined using an analytical method. By making use of boundary conditions, a characteristic eigen equation is derived for the proposed unconventional waveguide, which is used to plot the dispersion curves. In this analysis, we concentrate on the effect of the inner cladding width on the lowest cutoff value and propagation modes, and the findings of this theoretical study are discussed in details. Further, the obtained results are compared with those of Singh *el al.* [14] under similar conditions, and some insights are drawn. Propagation in such an unconventional double-clad waveguide is highly affected by the width of the inner cladding and it is demonstrated that the proposed waveguide can be operated in monomode.

Our main motivation is to study a new unconventional structure that gives new characteristics and insights so that some researchers interested for novel property of such unconventional waveguide for use in engineering and technology can choose this particular waveguide with desired property from the present investigation. However, the feasibility of fabrication, if not already there, is not remote in view of modern advances in nano-technology if only the experimentalists and practical engineers are sufficiently interested or encouraged to take up this sort of work [9].

2. Theoretical Formulation

The transverse section of a waveguide having a core refractive index n_1 and cladding refractive index n_2 (such that n_1-n_2 is very small) is shown in Fig. 1(a) and its index profile is shown in Fig.1 (b). For weakly guiding fibers, all the modes having same cut-off V-values degenerate, i.e, their $b-V$ curves almost merge. In weakly guiding situation there is substantial spread of fields in the cladding. The optical energy is not tightly confined to the core and is weakly guided. Here, we cannot identify the nature and kind of modes but on the basis of no. of modes and cutoff V-value we can investigate the modal propagation characteristics with some approximation [7].

The shape of the spiral is represented by the equation

$$r = \xi\theta, \tag{1}$$

where ξ is a size parameter.

To obtain the appropriate coordinates, one can use the points of intersection of two sets of normal curves in the cross-sectional plane of the waveguide. Now, the equation representing the normal curve can be written as

$$r = \eta e^{\frac{-\theta}{2}} \tag{2}$$

where η is a new parameter.

We omit some straightforward steps and obtain the scale factors: h_1, h_2, and h_3 for the coordinates ξ and η as follows:

$$h_1 = \frac{r\theta}{\xi\left(\theta^2+1\right)^{\frac{1}{2}}}; \qquad h_2 = \frac{r}{\eta\left(\theta^2+1\right)^{\frac{1}{2}}} \ ; \text{ and } \ h_3 = 1 \ ;$$
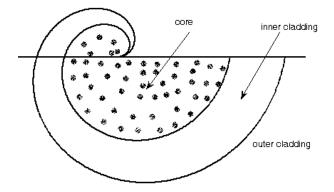

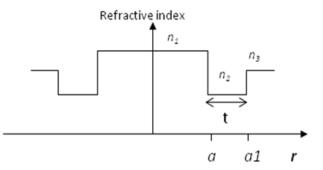*Fig. 1(a). The cross-sectional geometry of the proposed waveguide*

Fig. 1(b). Refractive index profile of the waveguide under consideration

where

$$r = \frac{\xi}{2}\ln\frac{\eta}{\xi} + \frac{3\xi}{4} \quad \text{and} \quad \theta = \frac{1}{2}\ln\frac{\eta}{\xi} + \frac{3}{4}.$$

Thus,
$$h_1 = \frac{\left(\frac{1}{2}\ln\frac{\eta}{\xi} + \frac{3}{4}\right)^2}{\left[\left(\frac{3}{4} + \frac{1}{2}\ln\frac{\eta}{\xi}\right)^2 + 1\right]^{\frac{1}{2}}};$$

$$h_2 = \frac{\xi}{\eta} \frac{\left(\frac{1}{2}\ln\frac{\eta}{\xi} + \frac{3}{4}\right)}{\left[\left(\frac{3}{4} + \frac{1}{2}\ln\frac{\eta}{\xi}\right)^2 + 1\right]^{\frac{1}{2}}}; \qquad \text{and} \quad h_3 = 1.$$

The scalar Helmholtz equation is given by

$$\nabla^2\psi + \omega^2\mu\varepsilon_1\psi = 0, \qquad (3)$$

where

$$\nabla^2 = \frac{1}{h_1 h_2 h_3}\left[\frac{\partial}{\partial a}\left(\frac{h_2 h_3}{h_1}\frac{\partial}{\partial a}\right) + \frac{\partial}{\partial c}\left(\frac{h_1 h_3}{h_2}\frac{\partial}{\partial c}\right) + \frac{\partial}{\partial z}\left(\frac{h_1 h_2}{h_3}\frac{\partial}{\partial z}\right)\right]$$

And ψ is the scalar approximation of any one of the cartesian components of the electric and magnetic fields. Proceeding further with this differential equation would be tedious unless some assumption is made for simplifications. If we choose $\eta \to \xi$, we have a manageable special case. Here, ω is a angular frequency, ε_1 is the permittivity of the guiding region (core) and μ is the permeability. Using this assumption in equation (3), the modified differential equation is given by

$$\frac{4\xi^2}{3}\frac{\partial^2\psi}{\partial\xi^2} + \frac{4\xi}{3}\frac{\partial\psi}{\partial\xi} + \frac{3\eta^2}{4}\frac{\partial^2\psi}{\partial c^2} +$$
$$\frac{3\eta}{4}\frac{\partial\psi}{\partial c} + \frac{27\xi^2}{100}\frac{\partial^2\psi}{\partial z^2} + \frac{27\xi^2}{100}\omega^2\mu\varepsilon_1\psi = 0. \qquad (4)$$

The technique of separation of variables will now be applied to obtain a solution as given in equation (4). We can obtain a solution for ψ in terms of η and ξ; that is,

$$\psi = E_1(\xi).E_2(\eta)\exp(j(\omega t - \beta z)) \qquad (5)$$

where β is the propagation constant along z-direction.

After a few steps, we obtain three equations, each of which is in one variable as

$$\eta\frac{\partial^2 E_2(\eta)}{\partial\eta^2} + \frac{\partial}{\partial\eta}E_2(\eta) = 0 \qquad (6)$$

$$\xi^2\frac{\partial^2 E_1(\xi)}{\partial\xi^2} + \xi\frac{\partial}{\partial c}E_1(\xi) + \frac{81}{400}U^2 E_1(\xi) = 0 \quad (7)$$

$$\xi^2\frac{\partial^2 E_1(\xi)}{\partial\xi^2} + \xi\frac{\partial}{\partial c}E_1(\xi) - \frac{81}{400}W^2 E_1(\xi) = 0, \quad (8)$$

where $\quad U = \sqrt{k_0^2 n_1^2 - \beta^2}; \quad W = \sqrt{\beta^2 - k_0^2 n_2^2}$ and

$$k_0 = \frac{2\pi}{\lambda_0}.$$

Equation (7) is valid for the guiding region and equation (8) for the cladding regions, respectively. Using new symbols

$$E_1(\xi) = y.\frac{81}{400} = p^2,$$

$\xi = x$ in Eqs. (7) and (8), and we have

$$x^2 y'' + xy' + p^2 U^2 \xi^2 y = 0 \qquad (9)$$
$$x^2 y'' + xy' + p^2 W^2 \xi^2 y = 0. \qquad (10)$$

Hence the axial field components for the proposed waveguide in various regions can be written as

$$E_{core} = AJ_0(pu\xi), \qquad \text{for core region} \qquad (11)$$

$$E_{cladI} = BI_0(pw_1\xi) + CK_0(pw_1\xi), \text{ for inner cladding region} \qquad (12)$$

$$E_{cladII} = DK_0(pw_2\xi), \text{ for outer cladding region} \qquad (13)$$

where $\quad u^2 = \omega^2 n_1^2\mu_1 - \beta^2, \quad w_1^2 = \beta^2 - \omega^2\mu_2 n_2^2$ and $w_2^2 = \beta^2 - \omega^2\mu_3 n_3^2$.

Matching the fields at the boundaries x = a and x = a$_1$ as shown Fig. 1(a), we get

$$E_{core}\big|_{\xi=a} = E_{cladI}\big|_{\xi=a} \qquad (14a)$$

$$E_{cladI}\big|_{\xi=a_1} = E_{cladII}\big|_{\xi=a_1} \qquad (14b)$$

$$\frac{dE_{core}}{d\xi}\bigg|_{\xi=a} = \frac{dE_{cladI}}{d\xi}\bigg|_{\xi=a} \qquad (14c)$$

$$\frac{dE_{cladI}}{d\xi}\bigg|_{\xi=a1} = \frac{dE_{cladII}}{d\xi}\bigg|_{\xi=a1} \qquad (14d)$$

Now employing the corresponding expressions for the electromagnetic fields in different regions in Eq. (14), we get the following characteristic equation:

$$\begin{vmatrix} J_0(pua) & -I_0(pw_1a) & -K_0(pw_1a) & 0 \\ uJ_0'(pua) & -w_1I_0'(pw_1a) & -w_1K_0'(pw_1a) & 0 \\ 0 & I_0(pw_1a_1) & K_0(pw_1a_1) & -K_0(pw_2a_1) \\ 0 & w_1I_0'(pw_1a_1) & w_1K_0'(pw_1a_1) & -w_2K_0'(pw_2a_1) \end{vmatrix} = 0 \qquad (15)$$

This equation (15) is known as the eigen value equation or characteristics equation.

The prime (/) of above equation represents differential with respect to the argument. The dimensionless V-parameter or the normalized frequency parameter is introduced to incorporate the parameters n_1, n_2, n_3, a, a_1 and k_0, which may possibly have an effect on the propagation. We define this parameter as

$$V = k_0 a (n_1^2 - n_2^2)^{\frac{1}{2}}, \qquad (16)$$

where k_0 is vacuum wave number.

3. Results and discussion

The characteristic equation (15) contains all the information that can be obtained from this analysis, and represents the central key points of this investigation. Generally, the exact modal analysis for unconventional optical waveguide is formidable. However, a highly accurate approximation known as weak-guidance approximation, $\Delta = ((n_{core} - n_{cladding})/n_{core}) \ll 1$, where difference between core and cladding refractive indices is very less than 1, and Δ is usually less than 0.02; is used for the weakly guided modes. Such conditions in communication channels allow for making the mathematical analysis by the scalar wave equation in terms of the Cartesian components of the E- and H-fields. Although Δ is also less than 1 for strong-guidance, it may be closer to 1. Strong-guidance is important in illumination engineering, however weak-guidance approximation gives sufficient approximated important results, including the cut-off V-values and number of modes, useful for optical communications [22].

We illustrate features of the waveguide with the help of equation (15) by taking $n_1 = 1.50$, $n_2 = 1.45$, and $n_3 = 1.46$ under weak-guidance approximation. Here, free space wavelength is chosen as $\lambda_0 = 1.55 \mu m$. Next, we plot the L.H.S. of equation (15) against β by considering equally spaced β - values in the propagation range $n_1 k_0 > \beta > n_2 k_0$, for a fixed value of a. The intersections of the graph with the β-axis give the possible allowed values of β. This procedure is repeated for a large number of values of a, and the normalized propagation constant b' can be obtained by using the relation:

$$b' = \frac{\beta^2 / k^2 - n_2^2}{n_1^2 - n_2^2}$$

The successive zero crossings of a typical β versus graphs will correspond to the successive modes. We can now plot the V versus b graph for each mode. Here, V is a dimensionless-parameter defined by $V = \frac{2\pi}{\lambda_0} a (n_1^2 - n_2^2)^{\frac{1}{2}}$. These dispersion curves are shown in Figs. 2 to 7 for these modes. The cutoff values obtained from the eigen-value equation (15), for different values of thickness t of the inner cladding region, are also mentioned in Table 1. Now, we discuss some important features of the dispersion curves obtained in the present study. An interesting inference is that at t = 0.01 μm, the waveguide behaves as a single mode guide for a large value of V, viz., 12, and even for V=20, there are only three modes. `

Though narrow end in a cross-section is rarely visualized, wider end the cross-section is similar to that of a distorted slab waveguide consisting of curvature and flare. Therefore, it can be said that such a waveguide can be useful in the study of the tolerance behavior of deformed slab waveguide. As we increase the width t from .01 μm to $t = 2 \mu m$, the cutoff V-value also increases and waveguide behaves as a single mode guide up to V=13.8. The cutoff value is greater and such waveguide is highly appropriate for the single mode propagation, which is needed for the sake of simplicity in manufacturing process of such waveguides, and it can be useful as desired in the scientific area of communication. It is noted that cutoff frequencies increase with increase in the inner cladding width. Thus, this is an important feature of the proposed waveguide with an additional degree of freedom to control the cutoff frequencies.

Further, we make comparison of these results with those obtained by Singh *et al.* [14] under similar conditions at $t = .01 \mu m$. Comparing these values, we find that the cutoff V-values at $t = 0.01 \mu m$ are V=5.1530, V=12.229 and V=19.262, as obtained from Fig.2, are much larger than the cut V-values V=1.66, V=8.67, V=15.67 obtained by Singh *et al.* Hence we conclude that the cutoff V-value is highly affected by the width of the introduced inner cladding region. This is the most important insight of the waveguide that it provides an additional degree of freedom to control the cutoff frequencies as well as single mode operation according to our choice.

4. Conclusion

An analytical method with scalar wave approximation is employed to analyze the modal behavior of a double-clad Archimedean shaped optical waveguide. In

appropriate orthogonal coordinates, the boundary conditions under the weak-guidance approximation, are imposed to obtain a modal eigen value equation for the proposed waveguide. With the help of this equation, we plot dispersion curves and by comparing these curves, cutoff frequencies and number of modes are calculated and discussed. It is found that, as we increase the width t, the cutoff V-value also increases and waveguide offers a single mode up to V=13.8. An attempt has been made to compare our results obtained for such doubly clad optical waveguide with a single clad waveguide having the cross-section of the same type, under the similar conditions. It is noted that the double clad Archimedean spiral waveguide

provides larger cutoff frequencies. Most important point is that the inner cladding width can tailor the cutoff conditions of the waveguide within a certain limit. Hence one can say that such a waveguide can provide an additional degree of freedom to control the cutoff frequencies and single mode operation. Furthermore, it is recommended that such waveguide can be highly appropriate for single mode propagation, as desired in manufacturing of waveguide. Single mode operation can be useful in communication industry as they do not offer intermodal dispersion and having lower propagation losses and hence the waveguide can offer much beneficial at high data rates in long distance communication.

Table 1. The cutoff frequencies (cutoff V-values) of the waveguide under consideration for different values of thickness (t)

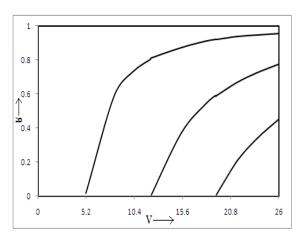| Cutoff V-value	t = 0.01μm	t=0.1 μm	t=0.2 μm	t=0.5 μm	t=1.0 μm	t=2.0 μm
V_1	5.1530	5.3629	5.5715	6.0508	6.4723	6.7120
V_2	12.229	12.417	12.617	13.102	13.560	13.827
V_3	19.262	19.447	19.644	20.136	20.606	20.882

Fig.2. Dispersion curves (b′ versus V) for the proposed waveguide for a few lowest modes under weak-guidance condition at t = 0.01μm.
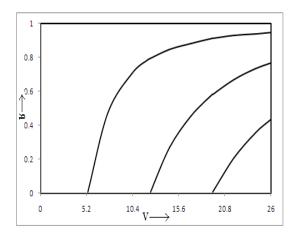

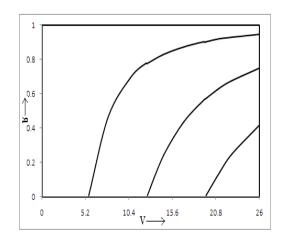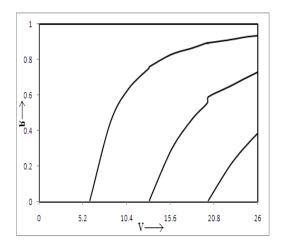*Fig. 4. Dispersion curves (b′ versus V) for the proposed waveguide for a few lowest modes under weak-guidance condition at t = 0.2μm.*
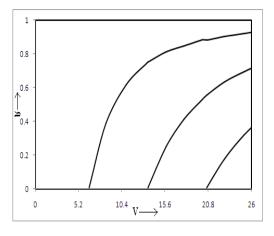

Fig.3. Dispersion curves (b′ versus V) for the proposed waveguide for a few lowest modes under weak-guidance condition at t = 0.1μm.

Fig. 5. Dispersion curves (b′ versus V) for the proposed waveguide for a few lowest modes under weak-guidance condition at t = 0.5μm.

Fig. 6. Dispersion curves (b$'$ versus V) for the proposed waveguide for a few lowest modes under weak-guidance condition at t = 1μm.

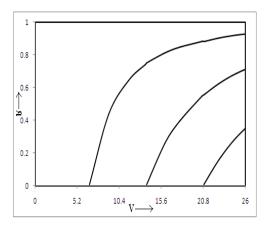*Fig.7. Dispersion curves (b$'$ versus V) for the proposed waveguide for a few lowest modes under weak guidance-condition at t = 2μm.*

References

[1] E. A. J. Marcatili, Bell. Syst. Tech. J. **48**, 2071 (1969).
[2] J.E. Goell, Bell Syst. Tech. J **48**, 2133 (1969).
[3] R.B. Dyott, Electron. Letts. **26**, 1721 (1990).

[4] C. Yeh, Optical and Quantum Electronics **8,** 43 (1976).
[5] V. Singh, B. Prasad, S. P. Ojha, Opt. Fiber Technol. **6,** 290 (2000).
[6] P. C. Pandey, B. K. Pandey, S. P. Ojha, Optik **5,** 211 (2000).
[7] N. Kumar, S. P. Ojha, Optik **124**, 773 (2013).
[8] S. N. Maurya, V. Singh, B. Prasad, S. P. Ojha, J. Electromagnetic Wave Appl. JEMWA **20**, 1021 (2006).
[9] V. Singh, Y. Prajapati, J. P. Saini, Prog. Eletromagnetic Res. PIER **64,** 191 (2006).
[10] A. Kumar, V. Thyagaranjan, A. K. Ghatak, Opt. Lett. **8,** 63 (1983).
[11] K. S. Chiang, IEEE Trans. Microw. Theory Tech. **37,** 349 (1991).
[12] V. Mishra, P. K. Choudhary, P. Khastgir, S. P. Ojha, Microwave Opt. Technol. Lett. **12,** 250 (1996).
[13] P. Sharan, P. Khastgir, P. K. Choudhury, S. P. Ojha, Photonics and Optoelctronics. **3,** 87 (1995).
[14] V. Singh, B. Prasad, S. P. Ojha, Optik **111**, 94 (2000).
[15] V. Singh, S. P. Ojha, L. K. Singh, Microwave Opt. Technol. Lett. **21**, 121 (1999).
[16] J. N. Polky, G. L. Mitchell, Opt. Soc. Am. **64,** 274 (1974).
[17] V. K. Varadan, A. Lakhtakia, V. V. Varadan, J. Wave-Mater Interact. **3,** 351 (1988).
[18] P. K. Choudhury, T. Yoshino, Optik. **115,** 49 (2004).
[19] A. V. Novitsky, L. M. Barkovsky, J. Opt A. Pure Appl. Opt. **7,** 51 (2005).
[20] N. Kumar, S. K. Srivastava, S. P. Ojha, Microwave Opt. Technol. Lett. **37,** 69 (2003).
[21] S. Kawakami, S. Nishida, Journal of Quantum Electronics, **QE-11,** 130 (1975).
[22] R. Jatan, R. Janma, V. Singh, N. Kumar, Optik **127,** 5761 (2016).
[23] A. W. Snyder, Understanding of monomode optical fibers, Proc. of IEEE. **69,** 6 (1981).
[24] A. Ghatak, A. Sharma, J. Inst. Electronics Telecom. Engrs. **32,** 213 (1986).
[25] T. Miya, K. Okamoto, Y. Ohmori, Y. Sasaki, IEEE J. Quantum Electronics **QE-17**, 858 (1981).
[26] A. Tomita, D. Marcuse, IEEE J. of Lightwave Technology, **LT-1,** 249 (1983).
[27] X. Song, R. Leonhardt, Progress in Electromagnetics Research, PIER **135**, 81 (2013).
[28] R. R. Grote, L. C. Bassett, APL Photonics **1**, 071302 (2016).
[29] S. Kawakami, M. Miyagi, S. Nishida, Applied Optics **14**, 2588 (1975).

_____
[*]Corresponding author: drjanmaphy @gmail.com